N O T I C E

THIS DOCUMENT HAS BEEN REPRODUCED FROM MICROFICHE. ALTHOUGH IT IS RECOGNIZED THAT CERTAIN PORTIONS ARE ILLEGIBLE, IT IS BEING RELEASED IN THE INTEREST OF MAKING AVAILABLE AS MUCH INFORMATION AS POSSIBLE

REPORT DOCUMENTATION PAGE

Form Approved
OMB No. 074-0188

Public reporting burden for this collection of information is estimated to average 1 hour per response including the time for reviewing instructions, searching existing data sources, gathering and maintaining the data needed and completing and reviewing this collection of information. Send comments regarding this burden estimate or any other aspect of this collection of information, including suggestions for reducing this burden to Washington Headquarters Services, Directorate for Information Operations and Reports, 1215 Jefferson Davis Highway, Suite 1204, Arlington, VA 22202-4302, and to the Office of Management and Budget, Paperwork Reduction Project (0704-0188), Washington, DC 20503

1. AGENCY USE ONLY (Leave blank)	2. REPORT DATE	3. REPORT TYPE AND DATES COVERED
	1991	Technical report, 1991

4. TITLE AND SUBTITLE
Two Years of Global Cirrus Cloud Statistics Using HIRS

5. FUNDING NUMBERS
ONR Grants N00014-85-K-0581 &
N00014-87-K-0436
NASA Grant NAG1-553
NSF Grant ATM-8703966
NOAA Contract 50-WCNE-8-06058
AFGL Grant F19628-91-K-0007

6. AUTHOR(S)
Donald Wylie, W. Paul Menzel, and H.M. Woolf

7. PERFORMING ORGANIZATION NAME(S) AND ADDRESS(ES)

University of Wisconsin-Madison
Space Science and Engineering Center

Satellite Application Laboratory,
NOAA/NESDIS
Madison, Wisconsin 53706

8. PERFORMING ORGANIZATION REPORT NUMBER
N/A

9. SPONSORING / MONITORING AGENCY NAME(S) AND ADDRESS(ES)

SERDP
901 North Stuart St. Suite 303
Arlington, VA 22203

10. SPONSORING / MONITORING AGENCY REPORT NUMBER
N/A

11. SUPPLEMENTARY NOTES
Submitted to the *Journal of Climate* on 23 August 1991. This work was supported in part by many various agencies & grants (see funding numbers). The United States Government has a royalty-free license throughout the world in all copyrightable material contained herein. All other rights are reserved by the copyright owner.

12a. DISTRIBUTION / AVAILABILITY STATEMENT
Approved for public release: distribution is unlimited

12b. DISTRIBUTION CODE
A

13. ABSTRACT ***(Maximum 200 Words)***

A climatology of upper tropospheric semi-transparent cirrus clouds has been compiled using HIRS multispectral infrared data, sensitive to CO_2 absorption, from the NOAA polar orbiting satellites. This is a report on the two years of data analyzed (June 1989 - May 1991). Semi-transparent clouds were found in 36% of the observations. Large seasonal changes were found in these clouds in many geographical areas; large changes occur in areas dominated by the ITCZ, the sub-tropical high pressure systems, and the mid-latitude storm belts. Semi-transparent clouds associated with these features move latitudinally with the seasons. These clouds also are more frequent in the summer hemisphere than the winter hemisphere. They appear to be linked to convective cloud development and the mid-latitudinal frontal weather systems. However, very thin semi-transparent cirrus has less seasonal movement than other cloud forms.

14. SUBJECT TERMS
HIRS multispectral infrared data, NOAA polar orbiting satellites, cirrus clouds, SERDP

15. NUMBER OF PAGES
37

16. PRICE CODE
N/A

17. SECURITY CLASSIFICATION OF REPORT	18. SECURITY CLASSIFICATION OF THIS PAGE	19. SECURITY CLASSIFICATION OF ABSTRACT	20. LIMITATION OF ABSTRACT
unclass	unclass	unclass	UL

NSN 7540-01-280-5500

Standard Form 298 (Rev. 2-89)
Prescribed by ANSI Std. Z39-18
298-102

DTIC QUALITY INSPECTED 1 19980817 115

2 - 1991

TWO YEARS OF GLOBAL CIRRUS CLOUD STATISTICS USING HIRS

Donald Wylie

Space Science and Engineering Center

University of Wisconsin-Madison

W. Paul Menzel and H. M. Woolf

Satellite Applications Laboratory

NOAA/NESDIS

Madison, Wisconsin 53706

Submitted to the Journal of Climate

23 August 1991

A 1

Abstract

A climatology of upper tropospheric semi-transparent cirrus clouds has been compiled using HIRS multispectral infrared data, sensitive to CO_2 absorption, from the NOAA polar orbiting satellites. This is a report on the two years of data analyzed (June 1989 - May 1991). Semi-transparent clouds were found in 36% of the observations. Large seasonal changes were found in these clouds in many geographical areas; large changes occur in areas dominated by the ITCZ, the sub-tropical high pressure systems, and the mid-latitude storm belts. Semi-transparent clouds associated with these features move latitudinally with the seasons. These clouds also are more frequent in the summer hemisphere than the winter hemisphere. They appear to be linked to convective cloud development and the mid-latitudinal frontal weather systems. However, very thin semi-transparent cirrus has less seasonal movement than other cloud forms.

1. Introduction

Cirrus clouds are crucially important to global radiative processes and the heat balance of the Earth; they allow solar heating while reducing infrared radiation to space. Models of climate changes will have to correctly simulate these clouds to have the proper radiative terms for the Earth's heat budget. Past estimates of the variation of cloud cover and the earth's outgoing longwave radiation have been derived primarily from the longwave infrared window (10-12 microns) radiances observed from polar orbiting and geostationary satellites (Rossow and Lacis, 1990; Gruber and Chen, 1988). The occurrence of semi-transparent clouds is often underestimated in these single

channel approaches. Recently, multispectral techniques have been used to better detect cirrus in global (Wu and Susskind, 1990) and North American (Wylie and Menzel, 1989) cloud studies.

This paper reports on the investigation of seasonal changes in the cirrus or semi-transparent global cloud cover with two years of multispectral observations from the polar orbiting HIRS (High resolution Infrared Radiation Sounder). Transmissive clouds that are partially transparent to terrestrial radiation have been separated from opaque clouds in the statistics of cloud cover (Wylie and Menzel, 1989). Semi-transparent or cirrus clouds are found in roughly 30 to 35% of all satellite observations.

The HIRS observations in the carbon dioxide absorption band at 15 microns have been used to calculate these cloud statistics. The CO_2 slicing algorithm calculates both cloud top pressure and effective emissivity from radiative transfer principles. Various CO_2 algorithms have been described in the literature (Chahine, 1974; Smith et al., 1974; Smith and Platt, 1978; Wielicki and Coakley, 1981; Menzel et al., 1983) and applications to data from the geostationary sounder VAS (VISSR Atmospheric Sounder) and the polar orbiting sounder HIRS have been published (Wylie and Menzel, 1989; Menzel et al., 1986; Susskind et al., 1987; Menzel et al., 1989; Eyre and Menzel, 1989).

2. Technique

Cirrus clouds often appear warmer in the window channel than the ambient air temperature at their altitude because they are transmitting radiation from below. This occurs in approximately 40% of the satellite data. The "CO_2 Slicing" technique is capable of detecting these clouds using the HIRS infrared channels with partial CO_2 absorption. It has the ability to distinguish partially transmissive clouds both during daylight and at night

and over either water or land backgrounds. The description of the technique, as applied to HIRS data, is presented in Menzel et al. (1989) and is repeated in Appendix A of this paper; it is similar to the application with VAS data described in Wylie and Menzel (1989). Cloud top pressure and effective emissivity are calculated for a given HIRS field of view (FOV).

Effective emissivity refers to the product of the fractional cloud cover, N, and the cloud emissivity, ϵ, for each observational area (roughly 30 km by 30 km). When $N\epsilon$ is less than unity, HIRS may be observing broken opaque cloud ($N<1$, $\epsilon=1$), overcast transmissive cloud ($N=1$, $\epsilon<1$), or broken transmissive cloud ($N<1$, $\epsilon<1$). All of these possibilities are labelled as "cirrus" in this paper. Cirrus usually are transmissive and exhibit spatial variations at scales ranging from hundreds of kilometers to smaller than the FOV of the instrument. Here, "cirrus" refers to an observation where the HIRS radiometer detects radiation from below a cloud layer as well as radiation from the cloud layer top. Effective emissivity observations less than 0.95 are labelled as cirrus while those greater than 0.95 are considered to be opaque clouds.

The technique is limited to finding the height of only the highest cloud layer in a multiple cloud layered situation. Cloud base altitude cannot be measured. Multiple layers often can be inferred from inspection of neighboring pixels where holes in the upper layer occur. Comparison to cloud reports from ground observers indicate that 50% of the time when the CO_2 technique detects an upper tropospheric cloud, one or more lower cloud layers also is present (Menzel and Strabala, 1989). Appendix B discusses the problems of the CO_2 slicing technique in multilayer cloud situations. For multilayer cloud situations where an opaque cloud underlies a transmissive cloud, the errors in the height of the transmissive cloud are about 100 mb too

low in the atmosphere for most cases. The error is largest when the underlying opaque layer is in the middle troposphere (400-700 mb) and smallest when the opaque cloud is near the surface or close to the transmissive layer. The error in effective emissivity increases as the opaque layer approaches the transmissive layer; when they are coincident the effective emissivity is set to one.

3. Global Cloud Statistics

A statistical summary of the global cloud observations from HIRS between June 1989 through May 1991 is shown in Table 1. Over 6 million observations were processed. The cloud top pressure determinations were subdivided into ten vertical levels from 100 mb to 1000 mb and effective emissivities were subdivided into five intervals from 0 to 1.00.

Table 1 reveals that high clouds above 400 mb comprised 20% of the observations. 30% of the observations were of clouds between 400 mb and 700 mb. Low clouds below 700 mb were found 22% of the time. Cloud free conditions were found 28% of the time.

Cirrus clouds (observations with effective emissivities less than 0.95) were found in 36% of our observations; they ranged from 100 to 700 mb. Clouds opaque to infrared radiation (observations with effective emissivities greater than 0.95) were found 36% of the time. The global average cloud amount (global average of $N\epsilon$) was found to be 0.53; Warren et al. (1988) report 0.61 from ground observations.

As the satellite views from above the atmosphere, high clouds were found in preference to low clouds. Broken low cloud fields were reported as opaque low clouds because of the technique's inability to sense the cloud fraction below the peaks in the CO_2 channels, as previously mentioned. The

transmissive clouds covered the range of effective emissivities from 0.0 to 0.95 fairly uniformly. Approximately 9% were found in each category.

As discussed in Menzel and Wylie (1991), the CO_2 slicing technique is subject to some errors. The large observation area (25 km by 25 km) produces results where the semi-transparent cloud observations are overestimated by roughly 5%. The HIRS lack of sensitivity to very thin clouds causes roughly 5% of the semi-transparent clouds to be incorrectly classified as opaque clouds of a lower altitude (Wylie and Menzel, 1989). Fortunately, these large errors are offsetting. Overall, because of the very large sample size and the relative accuracy of the CO_2 slicing technique, we claim that the entries in Table 1 are valid within 1%; all values should be interpreted as +/-0.5%.

A similar analysis of semi-transparent clouds was previously published for continental United States using GOES/VAS data (Wylie and Menzel, 1989, and Menzel et al., 1991). A comparison of the CO_2 slicing analysis of coincident data from both the GOES/VAS and NOAA/HIRS is shown in Appendix C. The two analyses produced similar statistics. However, the HIRS data produced more transmissive cloud observations than the VAS. We suspect that these differences appear because the FOV of the HIRS is larger than the VAS and the radiance noise of the HIRS is less than that of the VAS. The larger HIRS FOV reduces the ability of the HIRS to find breaks or holes in the upper level cloud fields. The VAS with a smaller FOV is able to report more of these holes whereas the HIRS averages them in with the cloud field. The smaller radiometric noise of the HIRS allows it to produce CO_2 slicing solutions more consistently. When observed and clear FOV radiance observations differ by less than the noise in the radiometric measurements, the algorithm avoids the CO_2 slicing solution and instead uses the window channel temperature to infer the cloud height for an opaque cloud (effective emissivity is set to 1.0).

These two differences in the HIRS and VAS would cause the HIRS to indicate more transmissive cloud than the VAS.

4. Seasonal and Geographical Trends

Figure 1 shows the winter and summer (referenced to the northern hemisphere) distribution of all clouds over land and ocean as a function of latitude. Winter refers to the months of December, January, and February; summer refers to June, July, and August. The seasonal summaries were compiled using a uniformly spaced grid of 2^{o} latitude by 3^{o} longitude. In each grid cell for each season, over 400 observations were made over the oceans and approximately 200 were made over land.

A large seasonal change was found over Antarctica, where few clouds of any altitude were reported in the summer (southern winter). The HIRS data do not show polar stratospheric clouds, which occur commonly over Antarctica in the months of June, July, and August. Polar stratospheric clouds apparently do not attenuate the HIRS channels sufficiently to mask out the strong inversions below them.

The remaining discussion will concentrate on the upper tropospheric clouds (above 500 mb). Figure 2 shows the zonal distribution of high clouds, which includes both the transmissive and opaque clouds (25% and 6% of all observations respectively). The frequent occurence of high clouds in the Inter-Tropical Convergence Zone (ITCZ) is prominent as the central maximum; the mid-latitude storm belts are evident in the secondary maxima. Seasonal shifts in the ITCZ are apparent over both land and ocean, as the ITCZ moves north and south with the sun. High clouds over land increase strongly from the equator to 30 S during the southern hemispheric summer (labelled as the northern winter). The high clouds over the southern hemispheric storm belt,

primarily over the oceans from 30 to 60 S, remain constant throughout the year. The northern hemispheric land masses from 45 to 75 N latitude also show little seasonal change in high cloud cover.

Figure 3 shows the geographical distribution of transmissive clouds in summer and winter (darker regions indicate more frequent cloud occurrence). The ITCZ is readily discernible as the band of more frequent cloud cover (darker band in the tropics). Again the ITCZ is seen to move north with the summer. The subtropical high pressure systems are also apparent as the band of less frequent cloud cover (white band in the subtropics). Cirrus clouds are less (more) frequent in the winter (summer) season in both hemispheres.

Over the Indonesian region the ITCZ expands in latitudinal coverage from winter to summer, enveloping the pocket of cloud minimum to the north. In the central Pacific, the ITCZ shows both a southern and northern extension during the winter months. In the southern hemisphere, the eastern Pacific ocean off of South America and the eastern Atlantic ocean off of Africa remain relatively free of transmissive cloud throughout the year.

The southern hemispheric storm belt (mentioned in the discussion of Figure 2) is evident throughout the year. In the northern hemisphere mid-latitude storm belts, the frequency of high clouds increased during the winter with the strengthening of the Aleutian Low in the north Pacific and the Icelandic Low in the north Atlantic. The cloud cover from both lows can be readily seen in the geographical plot (Fig. 3). The North American cirrus cloud cover shows little seasonal change agreeing with the GOES/VAS analysis (Wylie and Menzel, 1989).

Large convective development occurs during the winter (southern summer) in South America and Africa which is readily apparent through increased occurrence of high transmissive clouds. This explains the increase in high

cloud cover over land from the equator to 30 S during the winter (southern summer) evident in Figure 2.

Figure 4 shows the latitudinal distribution of thin transmissive (Nc less than .5) clouds for all seasons. The occurrence is slightly more likely over the ocean; this disagrees with Warren et al. (1988) who found more cirrus over land than ocean in their ground based observations. A modest peak from the equator to 10 N is evident both over land and ocean. Thin transmissive clouds appear globally with a frequency of 5 to 35%. Their seasonal movement was very small as shown in Figure 5. A slight increase was found in the southern hemisphere sub tropical high over oceans in the southern winter. A similar change was found over land in the sub-tropical deserts. The seasonal change in thin transmissive clouds is primarily occuring in the tropics.

5. Conclusions

There is a global preponderance of semi-transparent high clouds, presumed to be cirrus; 36% on the average for the two years covered by June 1989 to May 1991. In the ITCZ a high frequency of cirrus (greater than 50%) is found at all times; a modest seasonal movement tracks the sun. Large seasonal changes in cloud cover occur over the oceans in the storm belts at midlatitudes; the concentrations of these clouds migrated north and south with the seasons following the movement of convective systems (more cirrus is found in the summer than in the winter in each hemisphere). At higher latitudes cirrus were located with the cyclonic storms and frontal systems. At even higher latitudes, between 45 to 75, little seasonal change in cirrus is found. Over North America, cirrus show little seasonal change as they are found in regions of weak dynamics as well as strong. Thin cirrus exhibited even smaller seasonal changes.

Appendix A. Technique Description

The HIRS radiometer senses infrared radiation in eighteen spectral bands that lie between 3.9 and 15 microns at 25 to 40 km resolution (depending upon viewing angle) in addition to visible reflections at the same resolution. The four channels in the CO_2 absorption band at 15 microns are used to differentiate cloud altitudes and the longwave infrared window channel identifies the effective emissivity of the cloud in the HIRS field of view (FOV).

To assign a cloud top pressure to a given cloud element, the ratio of the deviations in cloud produced radiances, $R_{cld}(\nu)$, and the corresponding clear air radiances, $R_{clr}(\nu)$, for two spectral channels of frequency ν_1 and ν_2 viewing the same FOV can be written as

$$\frac{R_{cld}(\nu_1) - R_{clr}(\nu_1)}{R_{cld}(\nu_2) - R_{clr}(\nu_2)} = \frac{\epsilon_1 \int_{P_s}^{P_c} r(\nu_1,p) \frac{dB[\nu_1, T(p)]}{dp} dp}{\epsilon_2 \int_{P_s}^{P_c} r(\nu_2,p) \frac{dB[\nu_2, T(p)]}{dp} dp} . \quad (1)$$

In this equation, ϵ is the cloud emissivity, P_s the surface pressure, P_c the cloud pressure, $r(\nu,p)$ the fractional transmittance of radiation of frequency ν emitted from the atmospheric pressure level (p) arriving at the top of the atmosphere ($p = 0$), and $B[\nu,T(p)]$ is the Planck radiance of frequency ν for temperature $T(p)$. If the frequencies are close enough together, then ϵ_1

approximates ϵ_2, and one has an expression by which the pressure of the cloud within the FOV can be specified.

The left side of Eq. (1) is determined from the satellite observed radiances in a given FOV and the clear air radiances inferred from spatial analyses of satellite clear radiance observations. The right side of Eq. (1) is calculated from a temperature profile and the profiles of atmospheric transmittance for the spectral channels as a function of P_c, the cloud top pressure (1000 mb to 100 mb is spanned by discrete values at 50 mb intervals). In this study, global analyses of temperature and moisture fields from the National Meteorological Center (NMC) are used. The P_c that best matches observed and calculated ratios is the desired solution.

Once a cloud height has been determined, an effective cloud amount (also referred to as effective emissivity in this paper) can be evaluated from the infrared window channel data using the relation

$$N\epsilon = \frac{R_{cld}(w) - R_{clr}(w)}{B[w, T(P_c)] - R_{clr}(w)} . \qquad (2)$$

Here N is the fractional cloud cover within the FOV, $N\epsilon$ the effective cloud amount, w represents the window channel frequency, and $B[w, T(P_c)]$ is the opaque cloud radiance.

Using the ratios of radiances of the three CO_2 spectral channels, four separate cloud top pressures can be determined (14.2/14.0, 14.0/13.7, 14.0/13.3, and 13.7/13.3). Whenever $(R_{cld}-R_{clr})$ is within the noise response of the instrument (roughly 1 mW/m2/ster/cm-1), the resulting P_c is rejected. Using the infrared window and the four cloud top pressures, as many as four

effective cloud amount determinations can also be made. As described by Menzel (1983), the most representative cloud height and amount are those that best satisfy the radiative transfer equation for the four CO_2 channels.

If no ratio of radiances can be reliably calculated because (R_{cld}-R_{clr}) is within the instrument noise level, then a cloud top pressure is calculated directly from the comparison of the HIRS observed 11.2 micron infrared window channel brightness temperature with an in situ temperature profile and the effective emissivity is assumed to be unity. In this way, all clouds are assigned a cloud top pressure either by CO_2 or infrared window calculations.

Fields of view are determined to be clear or cloudy through inspection of the 11.2 micron brightness temperature with an 8.3 or 12.0 micron channel correction for moisture absorption. The channel differences (11.2 - 8.3 for NOAA 10 or 11.2 - 12.0 for NOAA 11) were used to lower the threshold for clear-cloudy decisions in areas were water vapor affected the window channel. This threshold change varied from 0 C near the poles in dry air masses to as high as 7 C in the moist tropical atmospheres. If the moisture corrected 11.2 micron brightness temperature is within 2 degrees Kelvin of the known surface temperature (over land this is inferred from the NMC Medium Range Forecast (MRF) model analysis; over the oceans this is the NMC sea surface temperature analysis), then the FOV is assumed to be clear (P_c = 1000 mb) and no cloud parameters are calculated.

The HIRS data were calibrated and navigated by NOAA/NESDIS. These data were transmitted daily to the Man computer Interactive Data Access System (McIDAS) at University of Wisconsin-Madison. The HIRS data from NOAA 10 and 11 were sampled to make the processing more manageable. Every third pixel on every third line was used. The data also were edited for zenith angle, eliminating data over 10° to minimize any problems caused by the increased

path length through the atmosphere of radiation upwelling to the satellite. It restricted the coverage to approximately the center one third of the orbit swath. With two satellites, about one half of the Earth is sampled each day.

Morning orbits over land also were rejected from the data because the surface temperature analysis over subtropical deserts was often warmer than the HIRS data; this caused cloud free areas to be mistaken as clouds. However, morning orbits over the oceans were used because no diurnal temperature change of the surface was assumed.

In the Arctic and Antarctic, the HIRS channels were inspected for the presence of surface temperature inversions. Over high altitude areas of Antarctica and Greenland, the HIRS 700 mb channel is often warmer than the window channel. We assumed that this indicated the presence of surface inversions from radiative cooling under clear skies. Surface inversions normally can not be seen by the HIRS because the 700 mb and window channels are looking at two distinctly different levels of the troposphere which have large temperature differences due to the prevailing lapse rates. However, over polar high altitude continents, the surface is closer to 700 mb and the inversions can be detected. When the 700 mb channel was warmer than the window channel, the observation was classified as cloud free. When isothermal conditions were found and the 700 mb channel was within 2 K of the window channel, we assumed that both channels saw the top of a cloud and the observation was classified as cloudy.

Appendix B. Errors associated with the presence of a lower cloud layer

The algorithm assumes that there is only one cloud layer. However, for over 50% of satellite reports of upper tropospheric opaque cloud, the ground observer indicates additional cloud layers below (Henzel and Strabala, 1989).

To understand the effects of lower cloud layers, consider the radiation sensed in a cloudy field of view. For a semi-transparent or cirrus cloud layer, the radiation reaching the satellite, R_{cld}, is given by

$$R_{cld} = R_a + \epsilon * R_c + (1-\epsilon) * R_b \qquad (3)$$

where R_a is the radiation coming from above the cloud, R_c is the radiation coming from the cloud itself, R_b is the radiation coming from below the cloud, and ϵ is the cloud emissivity. When a lower cloud layer is present under the semi-transparent or cirrus cloud, R_b is smaller (i.e., some of the warmer surface is obscured by the colder cloud). If prime indicates a two layer cloud situation of high semi-transparent cloud over lower cloud, and no prime indicates the single layer high semi-transparent cloud, then

$$R_b' < R_b, \qquad (4)$$

which implies

$$R_{cld}' < R_{cld}. \qquad (5)$$

Thus the difference of cloud and clear radiance is greater for the two layer situation,

$$[R_{clr} - R_{cld}'] > [R_{clr} - R_{cld}]. \qquad (6)$$

The effect of two cloud layers is greater for the 13.3 micron channel than for the other CO_2 micron channels, because the 13.3 micron channel "sees"

lower into the atmosphere (it has a non zero transmittance from low in the atmosphere). So using the 14.0/13.3 ratio as an example

$$[R_{clr}(13.3) - R_{cld}'(13.3)] > [R_{clr}(14.0) - R_{cld}'(14,0)]. \quad (7)$$

This reduces the ratio of the clear minus cloud radiance deviation in Eq. (1) because the denominator is affected more than the numerator (when the less transmissive channel is in the numerator),

$$\frac{[R_{clr}(14.0) - R_{cld}'(14.0)]}{[R_{clr}(13.3) - R_{cld}'(13.3)]} < \frac{[R_{clr}(14.0) - R_{cld}(14.0)]}{[R_{clr}(13.3) - R_{cld}(13.3)]}, \quad (8)$$

or L1' < L1, where L1 refers to the left side of Eq. (1). An example plot of P_c versus R1 (where R1 refers to the right side of Eq. (1)), shown in Figure 6, indicates that L1' < L1 implies $P_c' > P_c$. Thus, when calculating a cloud pressure for the upper semi-transparent cloud layer in a two cloud layer situation, the CO_2 slicing algorithm places the upper cloud layer too low in the atmosphere.

An example from 25 April 1991 is presented to illustrate further the magnitude of the errors that can be induced by lower level clouds (results for other days and other situations were found to be comparable). Observers in the Kwajalein Islands reported high cirrus clouds with no other underlying clouds present. The ratio of the 14.0 to 13.3 micron satellite observed radiance differences between clear and cloudy FOVs (the left side of Eq. (1)) is 0.41 on 25 April. This implies single layer cloud at 300 mb (solving the right side of Eq. (1) for P_c as shown in Fig. 6).

As explained above, if there had been an opaque cloud layer below 300 mb, R_{cld}' would have been smaller than measured for these cases. The changes in R_{cld}' were modelled for underlying opaque cloud layers at 850, 700, 600, 500, 400 and 300 mb (producing different ratios L1' in the left side of Eq. (1)). These changes will suggest different P_c' solutions as R1, the right side of Eq. (1), is matched to L1'. In the absence of any knowledge of a lower layer, the CO_2 algorithm integrates the right side of Eq. (1) from the surface to an incorrect P_c'. Figure 6 shows R1 as a function of P_c for the situation of 25 April. The errors in calculated cloud top pressure from the original 300 mb solution, $P_c' - P_c$, are shown as a function of height of the underlying opaque cloud layer in Figure 7 for 25 April.

In the two cloud layer situation, the position of the lower cloud layer affects the accuracy of the estimate of the height of the upper cloud layer. Opaque clouds in the lower troposphere near the surface underneath high cirrus have little affect on the cirrus P_c. The 14.2, 14.0, and 13.7 micron channels are not sensitive to radiation from low in the troposphere, but the 13.3 micron channel senses about one third of the radiation from below 800 mb. Opaque clouds in the middle troposphere, between 400 and 800 mb, underneath high cirrus, cause the cirrus P_c to be overestimated (lower in the atmosphere) by up to 190 mb (this extreme occurs for the very thin high cirrus cloud with N_ϵ of .10). The decreases in R_b produce smaller ratios for the left side of Eq. (1) which in turn produces larger estimates of P_c. Opaque clouds high in the atmosphere, underneath higher cirrus, have little effect on the cirrus P_c, since the height of the lower opaque layer approaches the height of the semi-transparent upper cloud layer and the CO_2 algorithm is going to estimate a height in between the two layers.

The errors in P_c were also examined for different emissivities of transmissive clouds (see Fig. 7). This was modelled by varying the emissivity in Eq. (3) and forming new ratios on the left side of Eq. (1). The maximum cloud top pressure error of roughly 190 mb occurred in very thin cloud with emissivity of .10. The error in P_c reduced as the emissivity of the transmissive clouds increased. For a cloud with emissivity of 0.5, the maximum error in P_c is about 60 mb. For more dense clouds with emissivity of 0.9, the maximum error in P_c is less than 10 mb. The satellite cloud data have shown a nearly uniform population of emissivity center around 0.5 (Wylie and Menzel, 1989), so one can conclude that the errors in the cloud top pressure caused by underlying clouds should average under 100 mb.

Multi-layer cloud situations (transmissive over opaque cloud) cause the height estimate of the upper cloud to be about 100 mb too low in the atmosphere on the average. The error in transmissive cloud height is largest when the underlying opaque layer is in the middle troposphere (400- 700 mb) and small to negligible when the opaque layer is near the surface or close to the transmissive layer. The error in effective emissivity increases as the opaque layer approaches the transmissive layer; when they are coincident, the effective emissivity is assumed to be one. These errors due to multi-layer clouds suggest that, overall, these HIRS estimates may be putting global clouds a little low in the atmosphere and with an effective emissivity a little too high.

Appendix C. Comparison of the NOAA/HIRS and the GOES/VAS cloud analyses.

The CO_2 Slicing Technique has been used to process cloud parameters with GOES/VAS data for four years prior to the start of the NOAA/HIRS analysis reported here (see Wylie and Menzel, 1989, and Menzel et al., 1991). The GOES/VAS algorithm uses the same equations as shown in Appendix A. However, there are small differences in the data and methods used in handling of the data. They are: (1) The GOES/VAS has three channels in the 13 to 15 micron region of the spectrum whereas the HIRS has four channels. (2) The GOES/VAS FOV (10 X 10 km) is smaller than the HIRS FOV (25 X 25 km); the VAS algorithm averages three FOV for each cloud determination representing 300 km^2, while the HIRS algorithm uses a single FOV representing approximately 625 km^2. (3) Surface topographic heights are used in the HIRS algorithm while they are not in the VAS algorithm; the surface pressure in Eq. (1) of Appendix A is determined from topography for the HIRS solutions while all VAS solutions assume a surface of 1000 mb. This affects the VAS results over the Rocky Mountains by 50 mb or less. (4) A separate sea surface temperature analysis is used in the HIRS processing while the VAS processing uses the same MRF model surface temperature analysis both over land and water. The VAS land surface temperatures are corrected using the SVCA hourly reports, whereas the HIRS are not. This will affect the determination of low cloud with the window channel, but it will have almost no effect on CO_2 algorithm solutions since only one of the channels sees the ground.

Two comparisons of HIRS and VAS cloud analyses were made. The first compared cloud parameter determinations for collocated HIRS and VAS FOVS. The second compared the seasonal average cloud frequencies for one summer and one winter. Table 2 shows the mean cloud height differences for collocated FOVs

from four separate days over Wisconsin in 1986. Cloud heights reported by the HIRS were 21 mb larger (lower altitude) on the average than the VAS in the single FOV comparison. Each day produced a different comparison. The average difference ranged from the HIRS being 73 mb smaller (higher altitude) than VAS on October 24 to being 76 mb larger (lower altitude) on October 28. All four days had transmissive clouds covering about 70% of the viewing area. Effective emissivities averaged 5 percent higher on the VAS than the HIRS. These differences are smaller than the estimated error (Menzel et al., 1991)

For the second comparison, the seasonal summaries of the first winter (December 1989 thru February 1990) and summer (June thru August 1989) of the HIRS analysis covering the area 26 to 50 N and 60 to 150 W were compared to the corresponding seasonal summaries of the VAS over the same area and time period. The geographical distribution of the probabilities of clouds above 700 mb in each season computed from VAS and HIRS are presented in Figure 8. Both the HIRS and VAS show a high probability of cloud cover over the northern Rocky Mountains in winter (about 80%), while they indicate a low probability (about 30% or less) in the southwest over Baja Mexico. In the summer, the cloud minima move northward into California on both the HIRS and VAS analyses. However, the HIRS reported a 30% probability of cloud cover (above 700 mb) in this minima in the summer while the VAS reported 10%. The HIRS also reported more clouds (above 700 mb) in the southeastern United States in summer and the Appalachian Mountains in winter.

A summary of all cloud reports from HIRS and VAS over the area 26-50 N and 60-150 W is shown in Table 3. The HIRS reported more semi-transparent cirrus in both winter and summer, 36% HIRS to 31% VAS in winter and 29% HIRS to 22% VAS in summer. In both seasons, the HIRS had 5 to 7% more cirrus observations than the VAS. The more frequent transmissive cloud reports of

the HIRS are thought to be partially caused by the larger sensor FOV of the HIRS than the VAS. The HIRS is unable to distinguish some high cloud areas which have spatial variations in effective emissivity. These areas are all categorized as transmissive cloud with HIRS while the smaller FOV of VAS allow separate identification of transmissive and opaque clouds.

When all transmissive and opaque high clouds above 400 mb were added together (second row of Table 3), the VAS found 10% more high clouds in the winter than the HIRS (29% VAS versus 19% HIRS) and 5% more in the summer (22% VAS versus 17% HIRS). The HIRS also found more middle level clouds between 400 and 700 mb than VAS (third row of Table 3), 31% HIRS compared to 22% VAS in winter and 26% HIRS to 16% VAS in summer. The HIRS and VAS found about the same amount of low level clouds (700 to 900 mb, fourth row in Table 3) in the winter, 29% VAS compared to 26% HIRS, and in the summer, 28% VAS and 29% HIRS. Considering clouds at all levels (rows two through four of Table 3), the HIRS sees slightly less cloud in the winter than the VAS (80% VAS to 76% HIRS) and more cloud in the summer (66% VAS to 72% HIRS).

In summary, the HIRS finds more mid-level clouds (400-700 mb) and fewer high level clouds than the VAS, but mostly agrees with it in low level cloud reports. The HIRS sees somewhat more semi-transparent clouds (5 to 10%) than the VAS. The vertical distribution of the clouds differs between the two instruments, but they have about the same percentage of cloudy observations.

Acknowledgments

This work was supported by Grants N00014-85-K-0581 and N00014-87-K-0436 of the Office of Naval Research and NAG1-553 from the National Aeronautics and Space Administration and Grant ATM-8703966 from the National Science Foundation and Contract 50-WCNE-8-06058 from the National Oceanic and

Atmospheric Administration and Grant F19628-91-K-0007 from the United States Air Force Geophysics Laboratory. The figures were prepared by Tony Wendricks.

References

Chahine, M. T., 1974: Remote sounding of cloudy atmospheres. I. The single cloud layer. J. Atmos. Sci., 31, 233-243.

Eyre, J. R., and W. P. Menzel, 1989: Retrieval of cloud parameters from satellite sounder data: A simulation study. J. Appl. Meteor., 28, 267-275.

Gruber, A., and T. S. Chen, 1988: Diurnal variation of outgoing longwave radiation. J. Clim. Appl. Meteor., 8, 1-16.

Menzel, W. P., W. L. Smith, and T. R. Stewart, 1983: Improved cloud motion wind vector and altitude assignment using VAS. J. Clim. Appl. Meteor., 22, 377-384.

Menzel, W. P., D. P. Wylie, and A. H.-L. Huang, 1986: Cloud top pressures and amounts using HIRS CO_2 channel radiances. Technical Proceedings of the Third International TOVS Study Conference, 13-19 August 1986, Madison, WI, 173-185.

Menzel, W. P. and K. I. Strabala, 1989: Preliminary report on the demonstration of the VAS CO_2 cloud parameters (cover, height, and amount) in support of the Automated Surface Observing System (ASOS). NOAA Tech Memo NESDIS 29.

Menzel, W. P., D. P. Wylie, and K. I. Strabala, 1989: Characteristics of global cloud cover derived from multispectral HIRS observations. Technical Proceedings of the Fifth International TOVS Study Conference, 24-28 July 1989, Toulouse, France, 276-290.

Menzel, W. P., Wylie, D. P., and Strabala, K. I., 1991: Seasonal and diurnal changes in cirrus clouds as seen in four years of observations with the VAS. Submitted to. J. of Appl. Meteor.

Rossow, W. B., and A. A. Lacis, 1990: Global and seasonal cloud variations from satellite radiance measurements. Part II: Cloud properties and radiative effects. J. Clim., in press.

Smith, W. L., H. M. Woolf, P. G. Abel, C. M. Hayden, M. Chalfant, and N. Grody, 1974: Nimbus 5 sounder data processing system. Part I: Measurement characteristics and data reduction procedures. NOAA Tech. Memo. NESS 57, 99pp.

Smith, W. L., and C. M. R. Platt, 1978: Intercomparison of radiosonde, ground based laser, and satellite deduced cloud heights. J. Appl. Meteor., 17, 1796-1802.

Susskind, J., D. Reuter, and M. T. Chahine, 1987: Cloud fields retrieved from analysis of HIRS/MSU sounding data. J. Geophys. Res., 92, 4035-4050.

Warren, S. G., C. J. Hahn, J. London, R. M. Chervin, and R. L. Jenne, 1988: Global distribution of total cloud over and cloud type amounts over the ocean. NCAR/TN-317+STR [Available from the National Center for Atmospheric Research, Boulder, CO, 80307]

Wielicki, B. A., and J. A. Coakley, 1981: Cloud retrieval using infrared sounder data: Error analysis. J. Appl. Meteor., 20, 157-169.

Wu, M. L. and J. Susskind, 1990: Outgoing longwave radiation computed from HIRS2/MSU soundings. J. Geophys. Res., 95D, 7579-7602.

Wylie, D. P., and W. P. Menzel, 1989: Two years of cloud cover statistics using VAS. J. Clim. Appl. Meteor., 2, 380-392.

Table 1: HIRS two year global cloud statistics (June 1989 to May 1991). The frequency of cloud observations for different heights and effective emissivities. Percentages are of the total number of observations, clear and cloudy combined. Clouds were not detected in 28% of the observations.

	ALL CLOUDS	EFFECTIVE EMISSIVITY				
LEVEL		≤0.25	≤0.50	≤0.75	≤0.95	>0.95
<200 mb	4%	1%	1%	0%	1%	1%
<300 mb	7	2	1	1	1	2
<400 mb	9	2	2	2	2	1
<500 mb	11	2	2	3	2	2
<600 mb	10	1	2	3	1	3
<700 mb	9	0	1	2	1	5
<800 mb	7	0	0	0	0	7
<900 mb	9	0	0	0	0	9
≤1000 mb	6	0	0	0	0	6
Total	72%	8%	9%	11%	8%	36%

Table 2: The mean cloud height differences for individual pixel comparisons between the HIRS and VAS over Wisconsin in the autumn of 1986.

Day	Time (UTC) HIRS	VAS	NOAA Satellite	Number of Comparisons	Cloud Top Pressure Difference HIRS-VAS
October 24, 1986	14:07	14:18	10	32	-35 mb
October 28, 1986	14:21	14:18	10	20	+76
October 31, 1986	20:26	20:18	9	29	+23
November 1, 1986	20:15	20:18	9	29	+42

Table 3: The frequency of cloud reports in the area 26 to 50 N and 60 to 150 W for the HIRS versus the VAS. Percentages are expressed as the fraction of all satellite observations in the area for the season, both cloud and clear combined. The winter included the months of December 1989 and January and February 1990. The summer included June through August of 1989.

	Winter		Summer	
Cloud Type	VAS	HIRS	VAS	HIRS
Semi-transparent cirrus	31 %	36 %	22 %	29 %
High clouds <400 mb	29	19	22	17
Middle clouds 400-700 mb	22	31	16	26
Low clouds >700 mb	29	26	28	29

Figure Captions

Figure 1: (a) The frequency of all clouds over ocean as a function of latitude for the summers (June, July, August) of 1989-90 and winters (December, January, February) 89-91 expressed as a fraction of all satellite observations, clear and cloudy combined. (b) The same over land.

Figure 2: (a) The frequency of high clouds, <500 mb, over ocean as a function of latitude for the summers (June, July, August) of 1989-90 and winters (December, January, February) 89-91 expressed as a fraction of all satellite observations, clear and cloudy combined. (b) The same over land.

Figure 3: (a) The geographic frequency of transmissive clouds for the summers (June, July, August) during the observation period June 1989 to May 1991. The left margin of the figure coincides with the International Date Line.

Figure 3: (b) The geographic frequency of transmissive clouds for the winters (December, January, and February) during the observation period June 1989 to May 1991.

Figure 4: The frequency of thin transmissive (Ne less than .5) over ocean and land as a function of latitude for the observation period June 1989 to May 1991 expressed as a fraction of all satellite observations, clear and cloudy combined.

Figure 5: (a) The frequency of thin transmissive (Ne less than .5) over ocean as a function of latitude for the summers (June, July, August) of 1989-90 and

winters (December, January, February) 89-91 expressed as a fraction of all satellite observations, clear and cloudy combined. (b) The same over land.

Figure 6: The calculated ratio from the right side of Eq. (1) as a function of cloud top pressure for the sounding of 25 April 1991 at the Kwajalein Island. The measured ratio from the left side of Eq. (1) is indicated. The cloud top pressure is inferred to be 300 mb.

Figure 7: (a) The errors in calculated cloud top pressure (from the original 300 mb solution) for several different Ne (0.1 to 0.9) as a function of height of the underlying opaque cloud layer.

Figure 7: (b) The errors in effective emissivity (from the original solution of Ne) as a function of height of the underlying opaque cloud layer.

Figure 8: The frequency of cloud observations (cirrus and opaque) that were reported at 700 mb and higher for the VAS and HIRS for one winter (Dec 89 - Feb 90) and one summer (June - August 89).

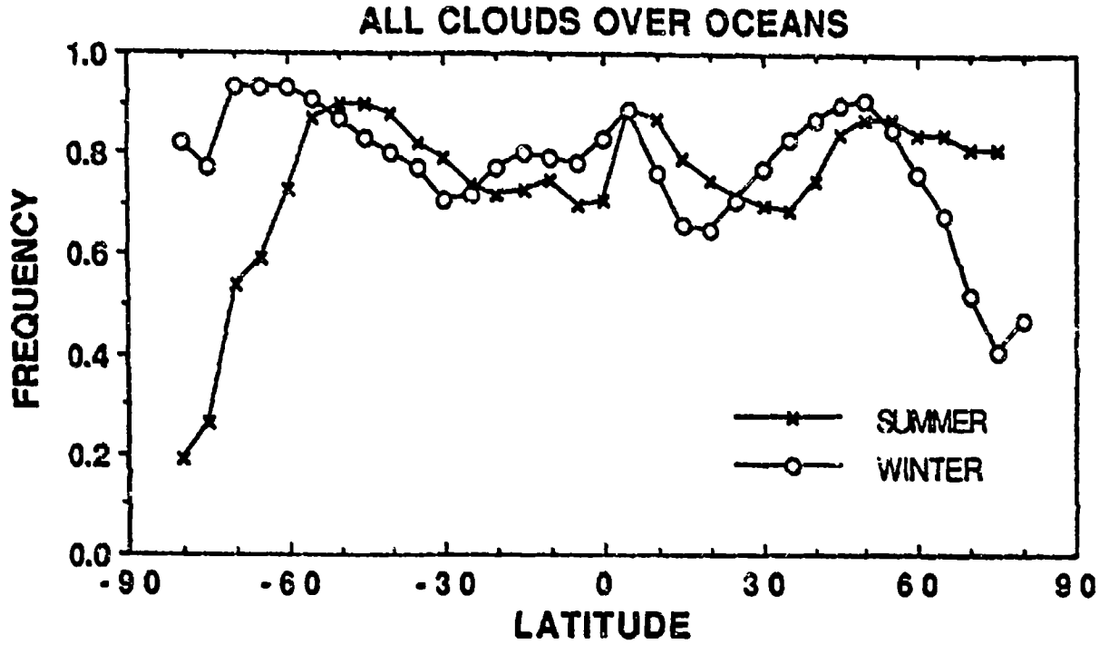

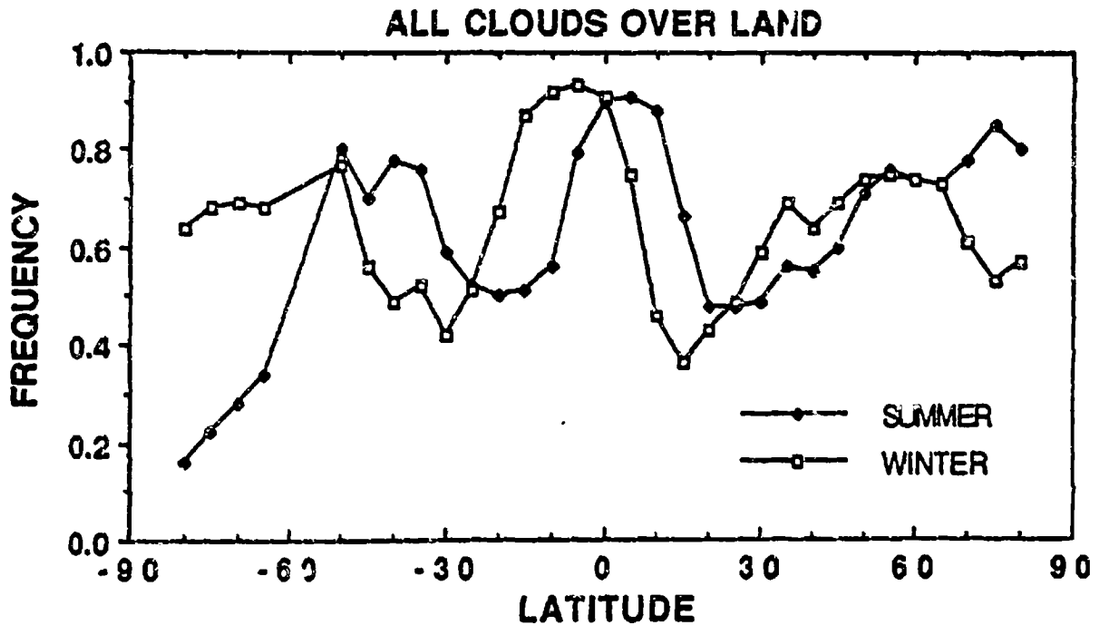

Figure 1: (a) The frequency of all clouds over ocean as a function of latitude for the summers (June, July, August) of 1989-90 and winters (December, January, February) 89-91 expressed as a fraction of all satellite observations, clear and cloudy combined. (b) The same over land.

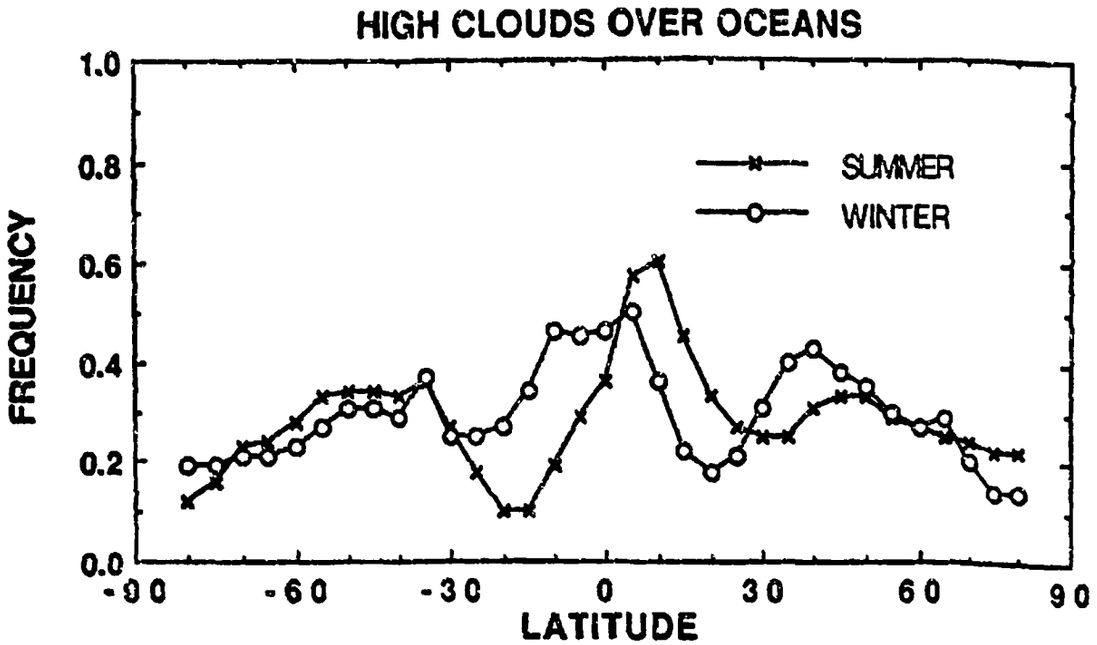

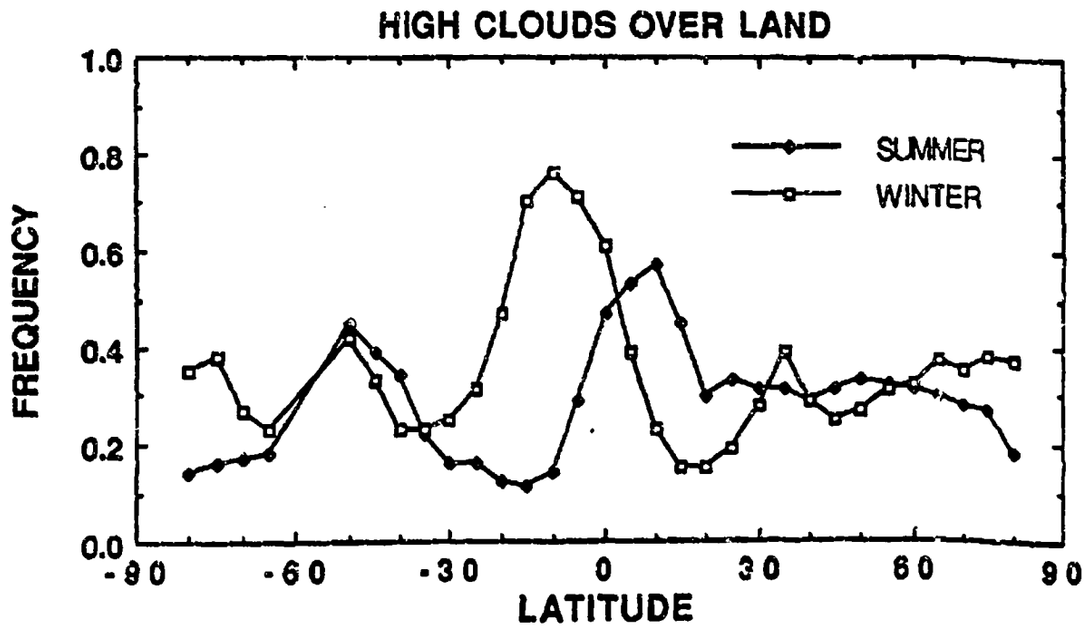

Figure 2: (a) The frequency of high clouds, <500 mb, over ocean as a function of latitude for the summers (June, July, August) of 1989-90 and winters (December, January, February) 89-91 expressed as a fraction of all satellite observations, clear and cloudy combined. (b) The same over land.

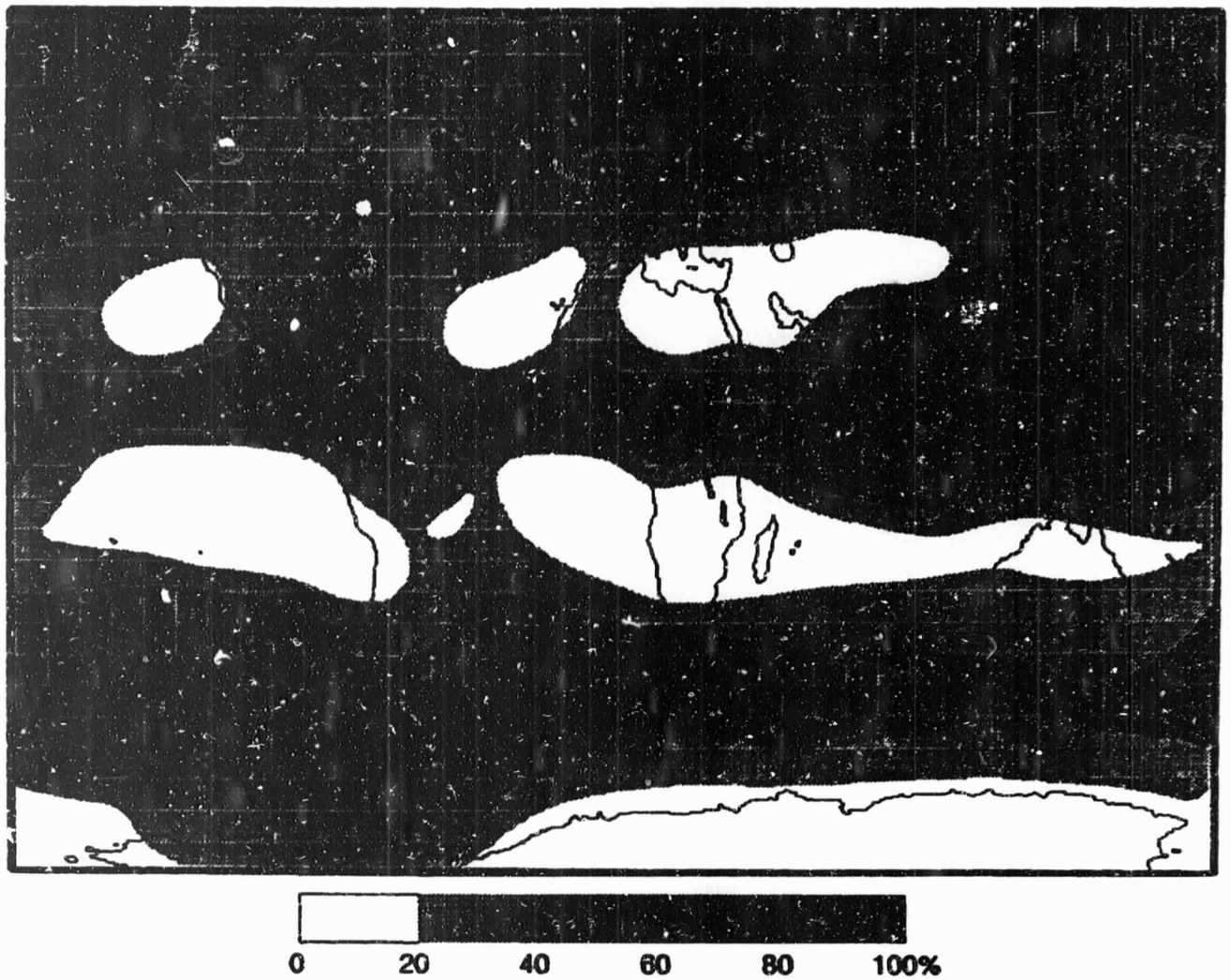

Figure 3: (a) The geographic frequency of transmissive clouds for the summers (June, July, August) during the observation period June 1989 to May 1991. The left margin of the figure coincides with the International Date Line.

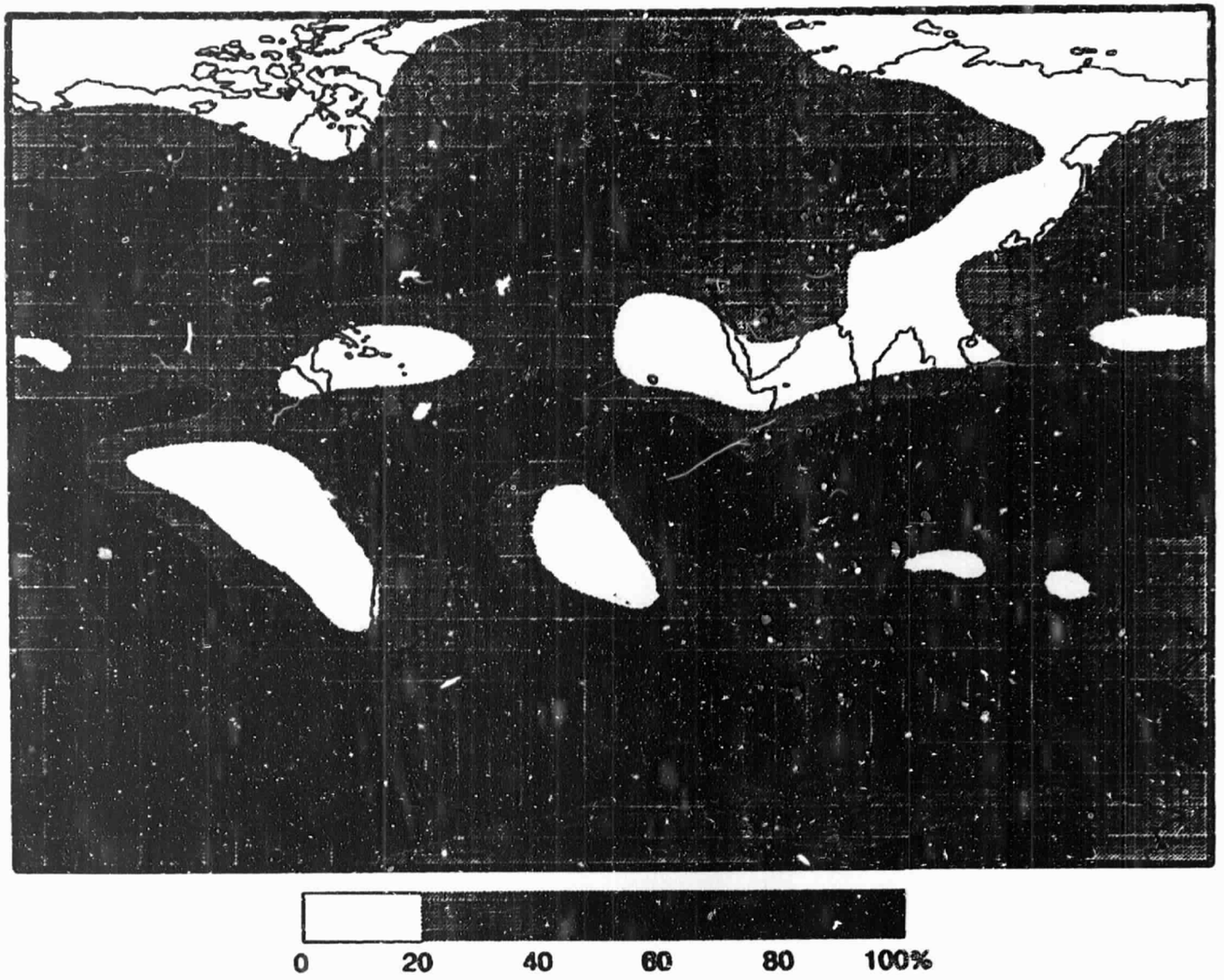

Figure 3: (b) The geographic frequency of transmissive clouds for the winters (December, January, and February) during the observation period June 1989 to May 1991.

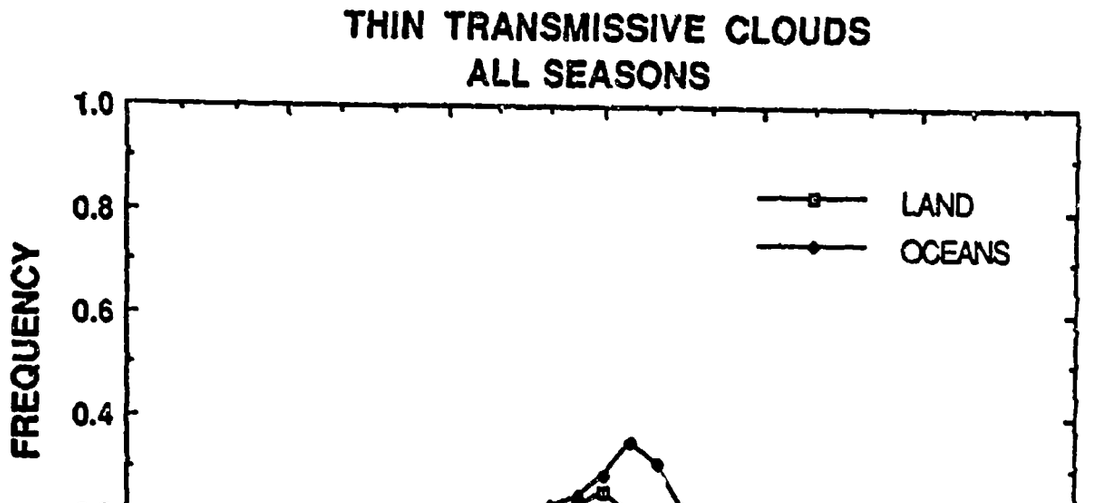

Figure 4: The frequency of thin transmissive (Nε less than .5) over ocean and land as a function of latitude for the observation period June 1989 to May 1991 expressed as a fraction of all satellite observations, clear and cloudy combined.

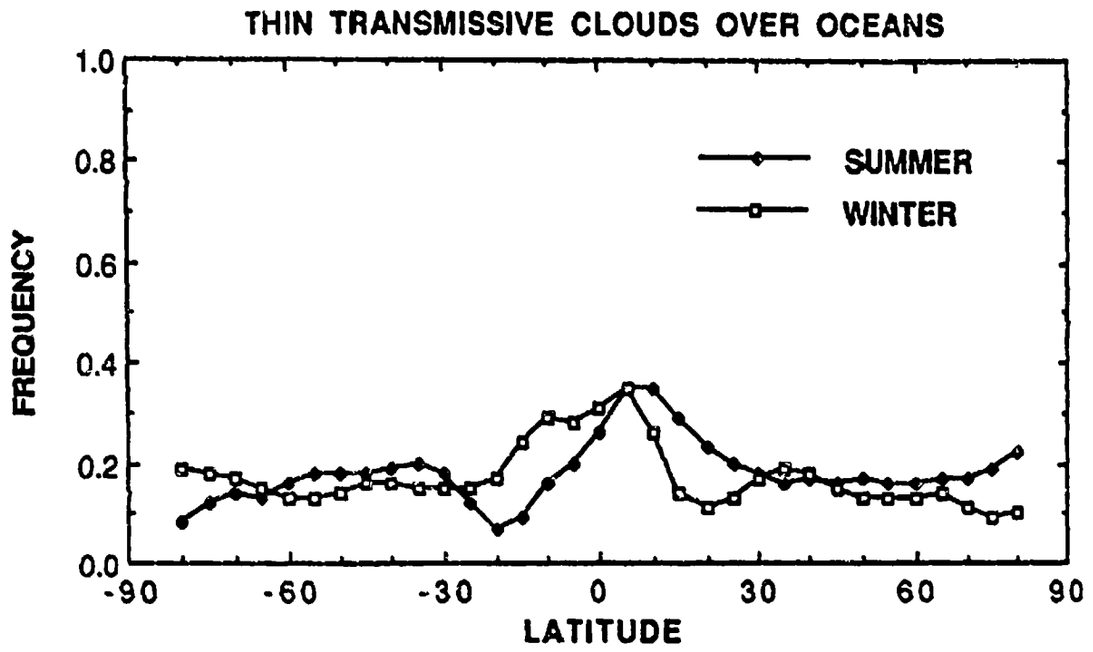

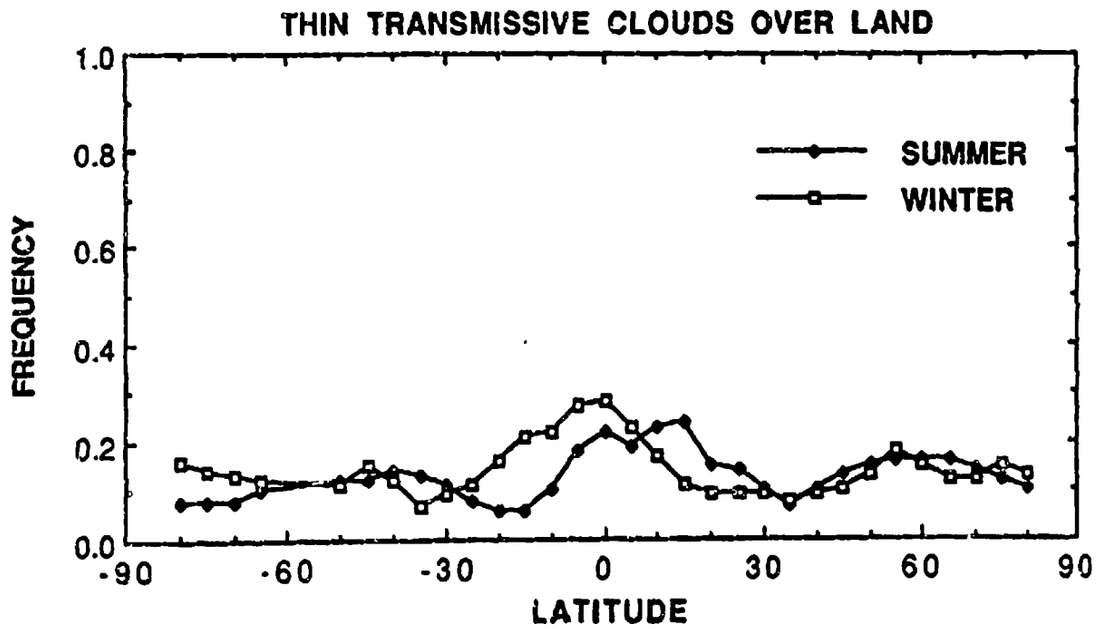

Figure 5: (a) The frequency of thin transmissive (N_c less than .5) over ocean as a function of latitude for the summers (June, July, August) of 1989-90 and winters (December, January, February) 89-91 expressed as a fraction of all satellite observations, clear and cloudy combined. (b) The same over land.

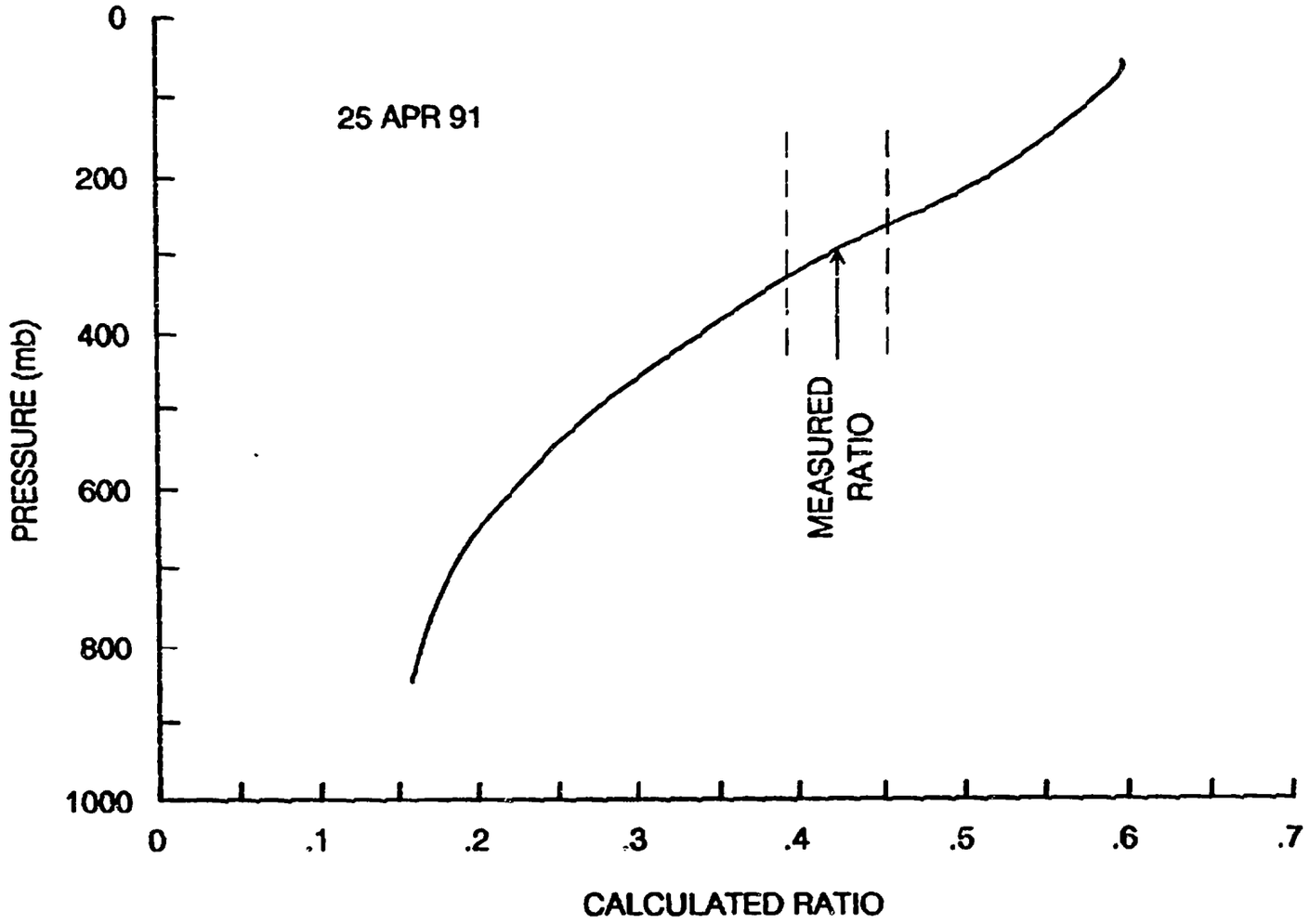

Figure 6: The calculated ratio from the right side of Eq. (1) as a function of cloud top pressure for the sounding of 25 April 1991 at the Kwajalein Island. The measured ratio from the left side of Eq. (1) is indicated. The cloud top pressure is inferred to be 300 mb.

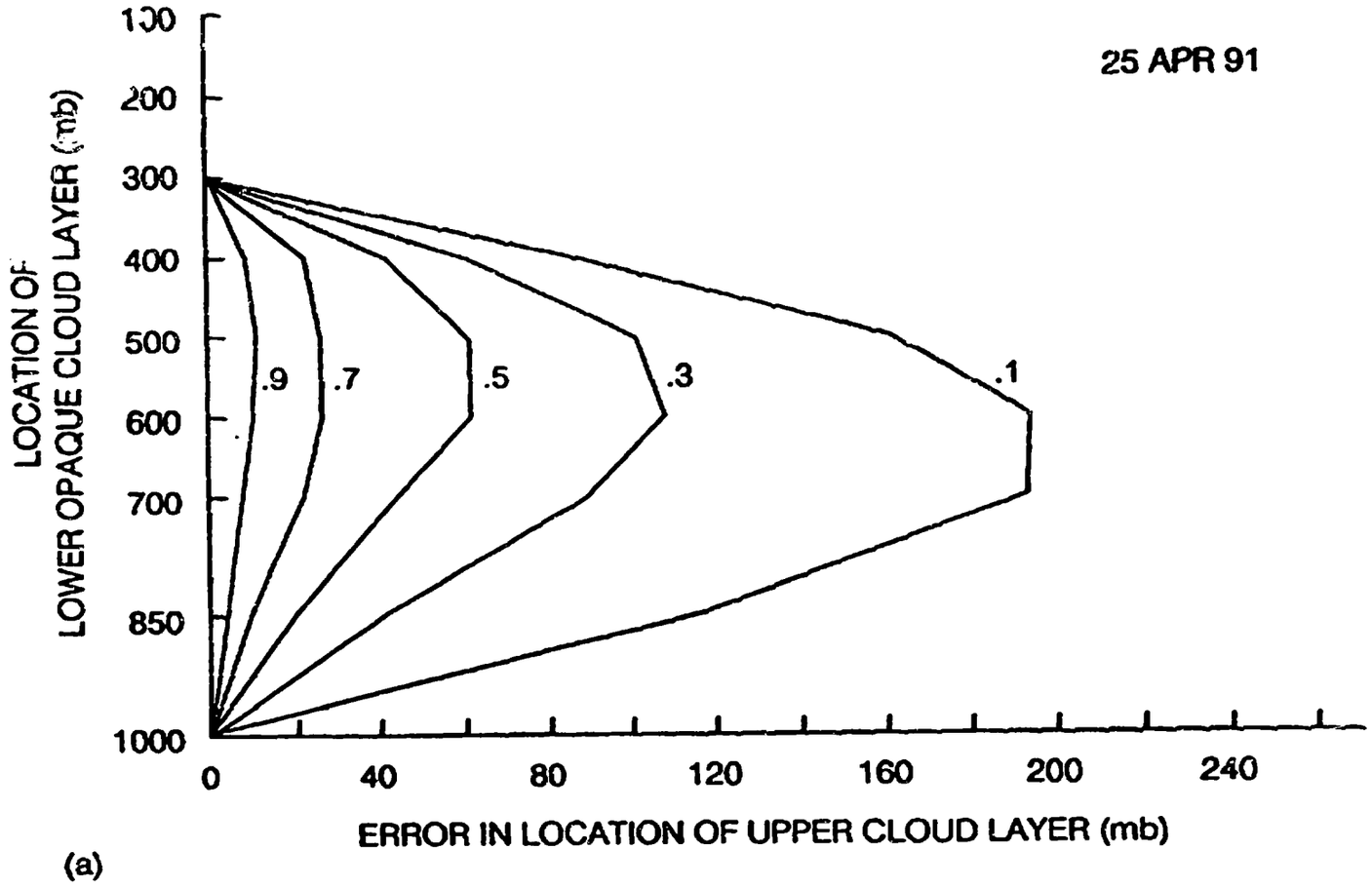

Figure 7: (a) The errors in calculated cloud top pressure (from the original 300 mb solution) for several different Ne (0.1 to 0.9) as a function of height of the underlying opaque cloud layer.

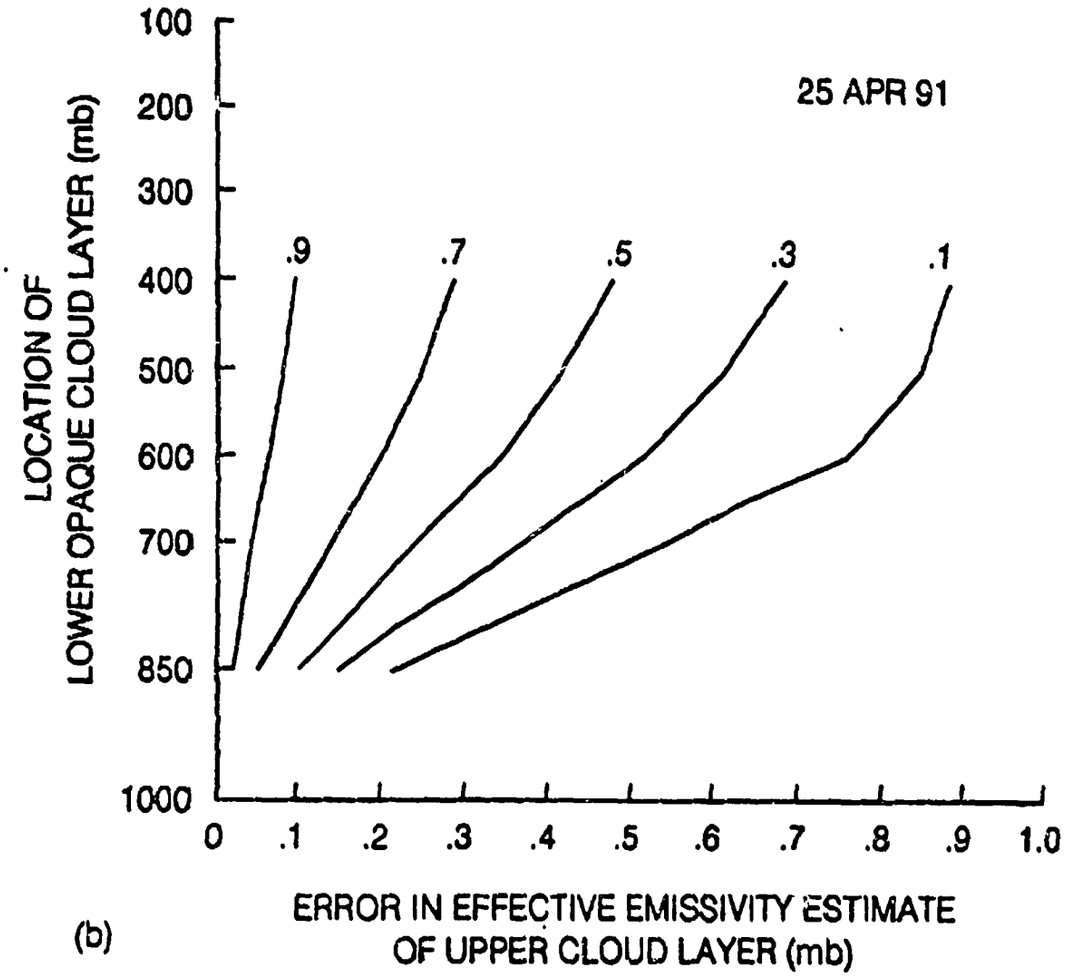

Figure 7: (b) The errors in effective emissivity (from the original solution of N_ϵ) as a function of height of the underlying opaque cloud layer.

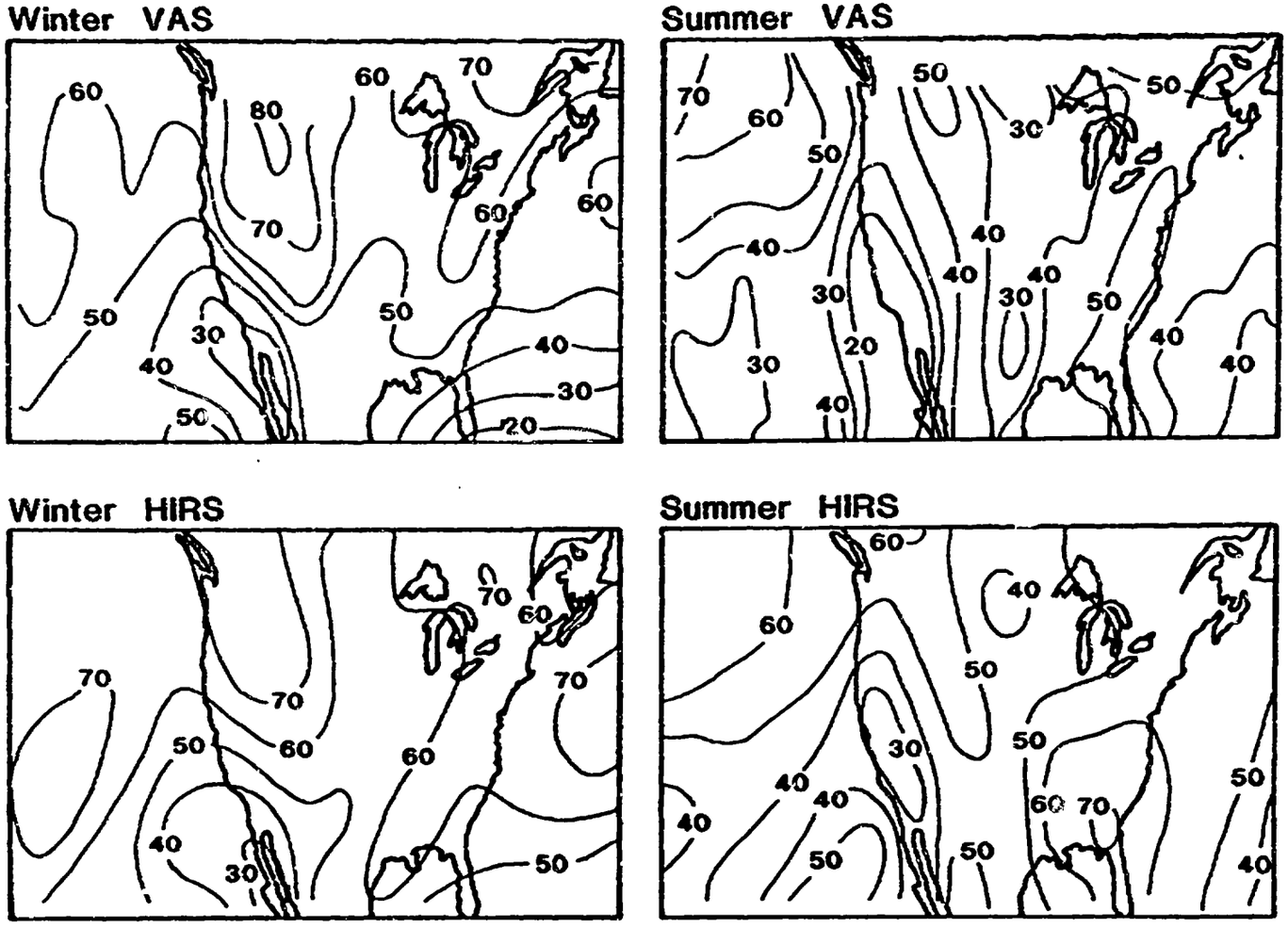

Figure 8: The frequency of cloud observations (cirrus and opaque) that were reported at 700 mb and higher for the VAS and HIRS for one winter (Dec 89 - Feb 90) and one summer (June - August 89).

REPRODUCTION QUALITY NOTICE

We use state-of-the-art high speed document scanning and reproduction equipment. In addition, we employ stringent quality control techniques at each stage of the scanning and reproduction process to ensure that our document reproduction is as true to the original as current scanning and reproduction technology allows. However, the following original document conditions may adversely affect Computer Output Microfiche (COM) and/or print reproduction:

- Pages smaller or larger than 8.5 inches x 11 inches.
- Pages with background color or light colored printing.
- Pages with smaller than 8 point type or poor printing.
- Pages with continuous tone material or color photographs.
- Very old material printed on poor quality or deteriorating paper.

If you are dissatisfied with the reproduction quality of any document that we provide, particularly those not exhibiting any of the above conditions, please feel free to contact our Directorate of User Services at (703) 767-9066/9068 or DSN 427-9066/9068 for refund or replacement.

END SCANNED DOCUMENT